Application of nonlinear wave modulation and break of reciprocity principle to assess corrosion-induced cracking in steel-reinforced concrete

M. Miró[1], J.N. Eiras[2], P. Poveda[3], M.Á. Climent[1], J. Ramis[3]

[1] Civil Engineering Department, University of Alicante, 03690 Sant Vicent del Raspeig, Alicante, Spain
m.miro@ua.es; ma.climent@ua.es
[2] Aix Marseille Univ, CNRS, Centrale Marseille, LMA, Marseille, France
jesus.eiras.fernandez@gmail.com
[3] DFISTS, University of Alicante, 03690 Sant Vicent del Raspeig, Alicante, Spain
pedro.poveda@ua.es; jramis@ua.es

Abstract

In this study, two ultrasonic testing techniques were used and compared to detect corrosion-induced cracking in prismatic mortar samples. Five specimens were prepared and subjected to accelerated corrosion conditions. The different times of exposure allowed to attain unalike damage conditions in every sample. Three out of five samples exhibited a visible crack at the end of the accelerated corrosion test (30 days). The onset of damage was monitored through the evolution of the accumulated Intensity Modulation Ratio (R) and crack width measurements. The accumulated values of the Intensity Modulation Ratio increased monotonically and clearly discriminated the five damage levels. Finally, once the specimens reached 5 different damage states, several reciprocity features were evaluated by using different ultrasonic testing configurations. The results proved that localized cracks cause a break of the reciprocity principle.

Keywords: Non-linear ultrasonic test, Cracks, Steel corrosion, Intermodulation products, Reciprocity.

1   Introduction

Corrosion-induced cracking is one of the most important causes of performance deterioration in reinforced concrete elements. Although various methods have been developed to detect the number and location of corrosion-induced cracks, sensitivity to closed small cracks located far below the concrete surface remains a problem to be studied. In only a few cases, nonlinear acoustic techniques have been applied in concrete corrosion tests under laboratory conditions [1-7]. Many of these earlier studies focus on the utility of the higher-order harmonic generation method to investigate corrosion-induced cracking in reinforced concrete samples [2, 5-7] and in different vibroacoustic modulation methods [2-4, 6]. Overall, the results were promising for the early detection of steel bar corrosion damage in reinforced concrete structures.
In this study, we further investigate the application of two nonlinear ultrasonic testing techniques for detecting the damage induced by steel corrosion in concrete.
Firstly, while the corrosion test was being performed, the technique used herein investigated the interaction of two monochromatic continuous waves at two separate frequency ranges, which is referred to as Nonlinear Wave Modulation Spectroscopy [8]. If a nonlinear system is excited by two signals of frequencies f_0 and f_1, referred to as pump (f_0) and probe (f_1) waves for $f_1 >> f_0$, the mechanical nonlinearity gives rise to additional output frequency components as sum and difference as $f_1 \pm n \cdot f_0$ (for n = 1, 2, …, N). Otherwise, if the system behaves linearly, the sideband frequencies are not generated. The amplitude of the sidebands with regard to

the amplitudes of the pump and probe waves enable the quantification of the nonlinear constitutive elastic properties [8] or the size of localized defects (cracks) if adequate modelling is available [9, 10]. Alternatively, in many studies a qualitative measure of the nonlinear behaviour is provided by comparing the relative strength of N sideband amplitudes with respect to the amplitude of the high-frequency probe A_1 as [11]:

$$R = \frac{\sum_{n=1}^{N}\left(A_{left}^{n} + A_{right}^{n}\right)}{A_1} \tag{1}$$

Secondly, at the end of the corrosion test, a series of measures based on the reciprocity principle were carried out. The presence of a localized nonlinearity in concrete not only breaks the proportionality between the input excitation and the output elastic response [12], but also affects the reciprocity of signals, the break of which turns out to be a nonlinear feature and to depend on the amplitude that excites the nonlinear scatterer.

It is well known from linear elasticity theory [13, 14] and diverse other fields [15-17] that the reciprocity principle, which represents the space and time invariance of elastic waves, holds true in linear media. This principle may be described as a nexus between a source and the detected elastic response of the excited medium[18]. In other words, the elastic response of the medium when injecting the same source function from position A and recording in position B is the same as the one recorded in A when injecting in B (see Figure 1.), with no dependence on the geometry of the sample [14]. The reciprocity principle has led to various applications, most of which concern imaging techniques based on ultrasonic/acoustic wave propagation [19].
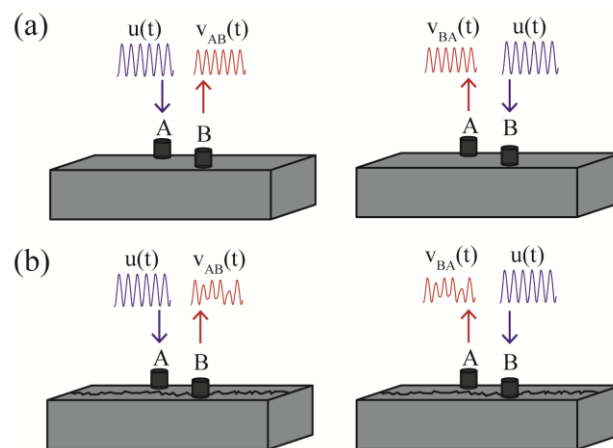
Figure 1 – Schematic representation of the reciprocity principle for elastic waves: (a) linear sample; (b) cracked sample [18].

In order to perform a qualitative analysis of the dependence of the loss of reciprocity on the nonlinear intensity with the degradation level, the definition of different amplitude-dependent indicators for the reciprocity is needed [20].

2   Experimental details

2.1   Materials and sample preparation

Five prismatic reinforced cement mortar specimens measuring 10 x 10 x 35 cm^3 and having identical composition were prepared. Standard siliceous sand (1350 g) and Portland cement type CEM I 52.5 R-SR 3 [21] (450 g) were used. The water to cement mass ratio (w/c) was set to 0.5 (225 g). An amount of sodium chloride was incorporated into the mortar mix to provide an equivalent content of 2% Cl$^-$, relative to the cement weight in the hardened mortar (14.8 g) [22]. The molds allowed center-crossing of one steel rebar of 12 mm in diameter along the longitudinal axis and placed at 25 mm of its bottommost surface (in contact with the mold). This layout was chosen to promote a longitudinal crack on the samples upon corrosion of the steel rebar. The steel rebars were previously cleaned from native corrosion products [23] and the ends of each rebar piece were covered with vinyl electrical tape to avoid the steel-mortar-air interface in the accelerated corrosion tests. The mortars were prepared [24], poured into the plastic molds, mechanically compacted, and cured for 28 days in a humidity chamber at 20 ℃ and 95% relative humidity. Once the samples were cured, accelerated corrosion tests were started.

2.2   Accelerated corrosion test and damage levels

The accelerated corrosion test was conducted using a potentiostat–galvanostat (Model 362, EG&G Instruments, Princeton NJ, USA). A constant anodic current density of 100 mA/cm^2 was applied between the steel rebar (anode) and an external galvanized steel grid (cathode) placed at the bottom of the specimens (see Figure 2).

To keep an appropriate electrical conductivity throughout the cement mortar, the samples were partially submerged (5 mm height) in a recipient filled with tap water (except the control sample which was preserved in ambient conditions). Given that the potentiostat–galvanostat provided a constant current density, it was possible to corrode four specimens simultaneously by connecting them in series. In the experimental conditions of these tests, the penetration of the steel corrosion process can be considered as linear with time being the corrosion rate equal to the anodic current density passing through the electric circuit (current efficiency 100%) [4, 7, 25].

The exposure time duration to accelerated corrosion conditions was chosen for each sample to attain a different level of degradation. One sample was preserved as reference (M0, Control), so it was not subjected to the passing current. The sample M1 was exposed 3 days before any crack appeared. The sample M2 was exposed 6 days, also with no visible damage. The first crack appeared after 6 days in the samples M3 and M4. At this time, the sample M3 was disconnected, while the M4 was exposed to the passing current up to completing 20 days, so further damage was generated.
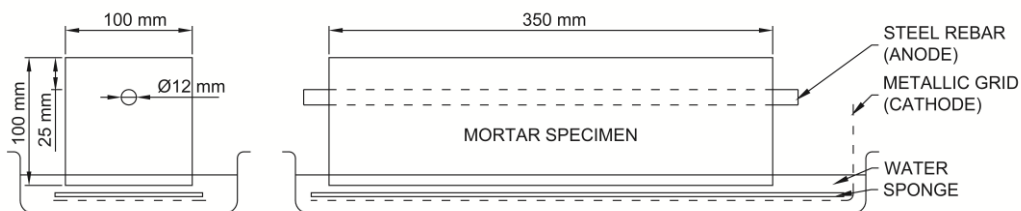
Figure 2 – Schema of the samples.

2.3 Non-linear ultrasonic measurements

2.3.1 Modulation

Figure 3 shows the experimental setup used for the ultrasonic measurements and the relative positions between emitting (EL and EZ) and receiving (RZ) transducers. The test was repeated at the three different positions shown in Figure 3. Two transducers were used to simultaneously supply two pure tones (f_0 = 20 kHz and f_1 = 200 kHz). The high-frequency probe signal was emitted with a signal generator (SONY AFG310) at an amplitude of 5 V. A 16- bit ADC resolution I/O device NI-USB 6361 was used for the generation of the low-frequency pump and the acquisition of the frequency modulated signal with a sampling frequency of 2 MHz.

The acquisition length was set to 50 ms. The pump wave signal was fed through an amplifier FS WMA-100 and then transmitted through a Langevin transducer. The input voltage was set to 130 V (after amplification). Two broadband ultrasonic transducers IDK09 [26] were used for emitting and receiving the high-frequency signal. White soft paraffin (Acofarma) was used as a coupling agent.

A Blackman window with a length of 35 ms was applied to the steady-state interval of the received signal and transformed to the frequency domain through the Fast Fourier Transform algorithm. Then, the amplitudes of the probe (A_{f1}) and the expected first- and second-order intermodulation frequencies ($A_{f1\pm f0}$ and $A_{f1\pm 2f0}$, say N was set to 2) were used to evaluate the nonlinear parameter R as defined in Eq. (1).
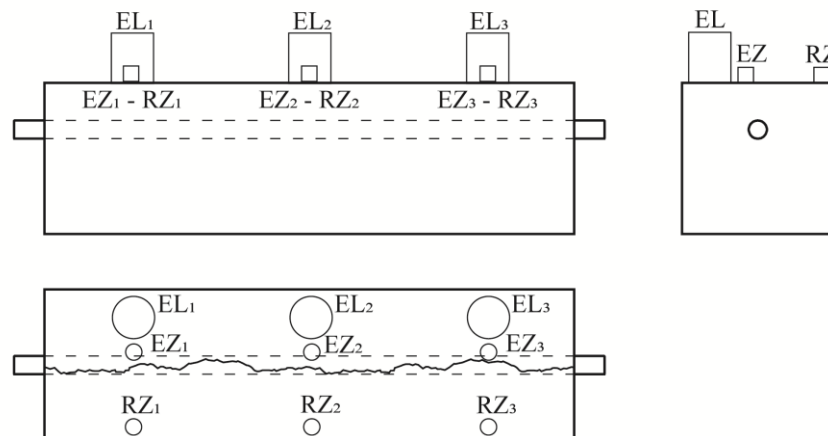
Figure 3 – Transducer positions 1, 2 and 3 of emitting Langevin transducers (EL), emitting IDK09[26] transducers (EZ) and receiving (RZ) transducers.

2.3.2 Reciprocity

Finally, at the end of the accelerated corrosion exposure, a comparison of the final condition was also made through reciprocity measurements on each sample. To this purpose, the samples were previously let dry in laboratory conditions. Then a reciprocity ultrasonic test (on two configurations) was performed. Figure 4 shows the two configurations (1 and 2) and the two positions (A and B) between emitting and receiving shear wave transducers (Panametrics), see Figure 4. A high viscosity coupling agent was used.
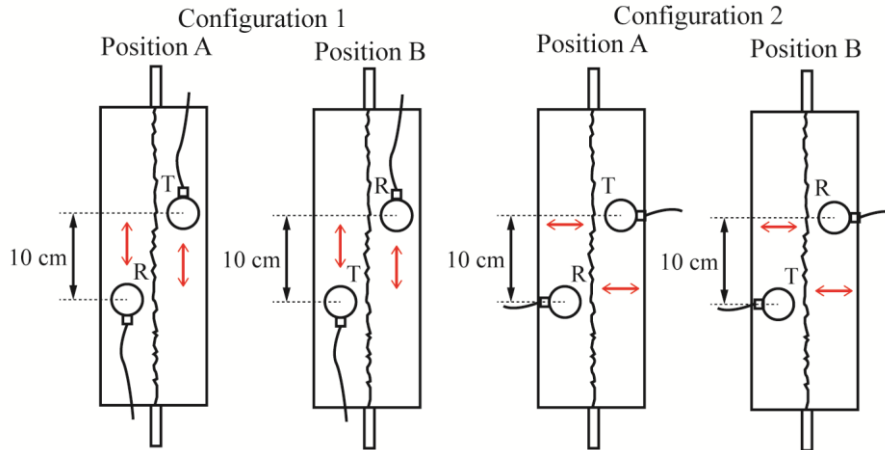
Figure 4 – Configurations (1 and 2) and positions (A and B) of the ultrasonic reciprocity measurements.

A pure tone signal was generated with a PC (WaveGen) and emitted by a transducer at a frequency of 250 kHz, varying the input amplitude A_i of the mechanical excitation. The amplitudes used were 10V, 25V, 50V, 75V, 100V, 125V and 150V. The received signal was sent to an amplifier High Voltage Pulser-Receiver (Panametrics Model 5058PR, Sofranel) [27] and bandpass filtered between 30 kHz and 1 MHz. The average of 100 signals were registered with an oscilloscope Teledyne Lecroy HDO4024A with a vertical resolution of 12 bits and a sampling frequency of 20 MHz.
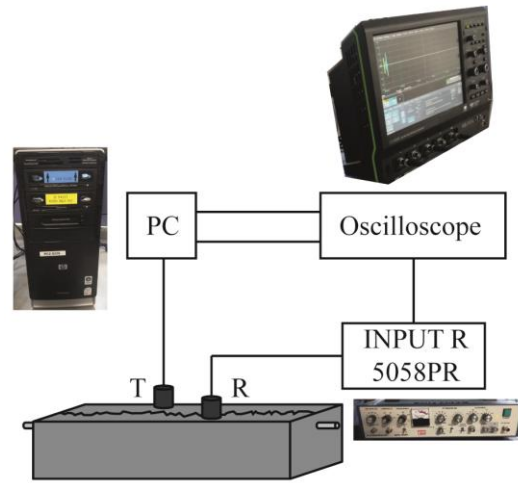
Figure 5 – Experimental setup used for the reciprocity ultrasonic measurements.

The indication of reciprocity was defined as the difference between the elastic responses v_{AB} and v_{BA}, of the signals generated by a transducer placed in position A and recorded in B and vice versa, at every fixed amplitude (A_i) of excitation [18]:

$$r^i = v^i_{AB} - v^i_{BA} \tag{2}$$

Moreover, a reciprocity parameter D^i can also be defined as the maximum of the reciprocity signal of Eq. (2) [18]:

$$D^i = \frac{2\max(r^i)}{\max(v^i_{AB}) + \max(v^i_{BA})} \tag{3}$$

The parameter D^i increases as the difference between waveforms v_{AB} and v_{BA} increases.

3   Results and discussion

Two different strategies were used to evaluate the potential of the intermodulation parameter R to detect the damage inflicted by the steel rebar corrosion. First, the evolution of the intermodulation parameter R was monitored over the accelerated corrosion test for 30 days. Second, measurements (on the two investigated configurations) were realized later to compare the final condition of the five samples.

For the monitoring test, two measurements were done before starting the accelerated corrosion test (henceforth, referred to as days -1 and 0). The analysis of the R values obtained at the undamaged condition did not show significant differences between the three investigated positions.

The nonlinearity parameter that is measured at each moment of the test would correspond to the microcracks (or their growth rate). Therefore, a cumulative value (that is, the area under the non-linearity parameter versus time) would roughly represent the more generally defined crack damage state [28]. Figure 6 shows the variation of the R parameter accumulated over time for the 5 study specimens. The accumulated R parameter clearly shows a distinction between the control specimen (Sample 0), the uncracked specimens (Samples 1 and 2), and the cracked specimens (Samples 3 and 4). Therefore, the cumulative nonlinearity parameter can be used to discern different levels of corrosion damage and cracking.
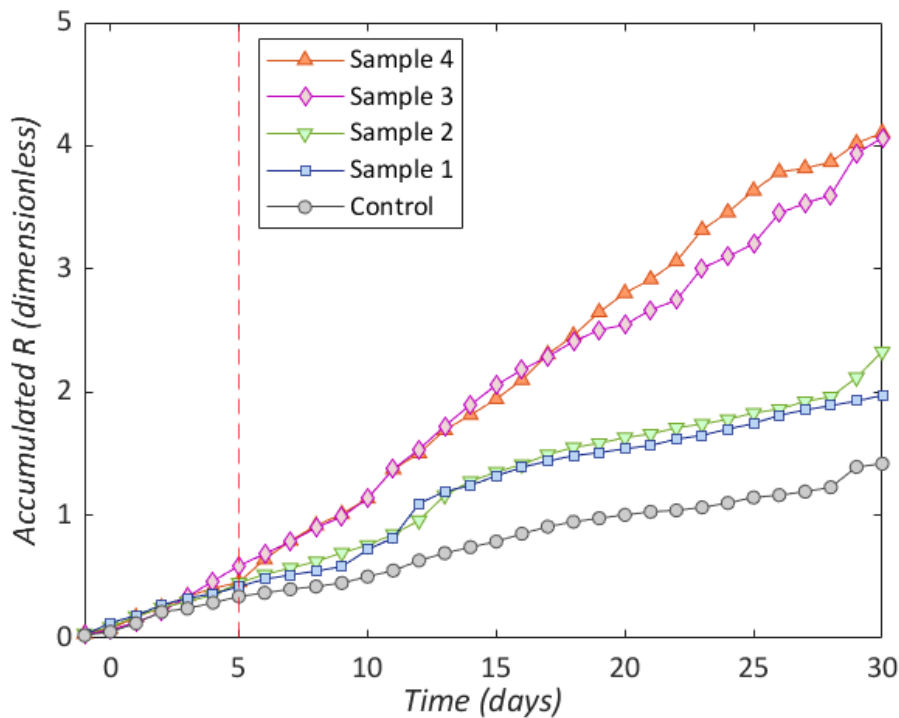
Figure 6 – Evolution over time of the non-linear parameter R accumulated for each reinforced mortar specimen.

Figure 7 shows the superposition of supposedly reciprocal signals for the maximum amplitude (150V). The black solid line refers to the signal recorded in B when emitting from A, while the dashed red line refers to signals recorded in A when emitting from B. Figures 7(a) and 7(b) are signals detected in the Control sample (undamaged) and plots in Figures 7(c) and 7(d) are relative to the Sample 1 (damaged). Figures 7(a) and 7(c) are the superposition of signals recorded in Configuration 1 Figures 7(c) and 7(d) are the superposition of signals recorded in Configuration 2, see Figure 4. These results reveal that reciprocity breaks only in the sample damaged while the control sample shows a linear behaviour.

Configuration 1   Configuration 2
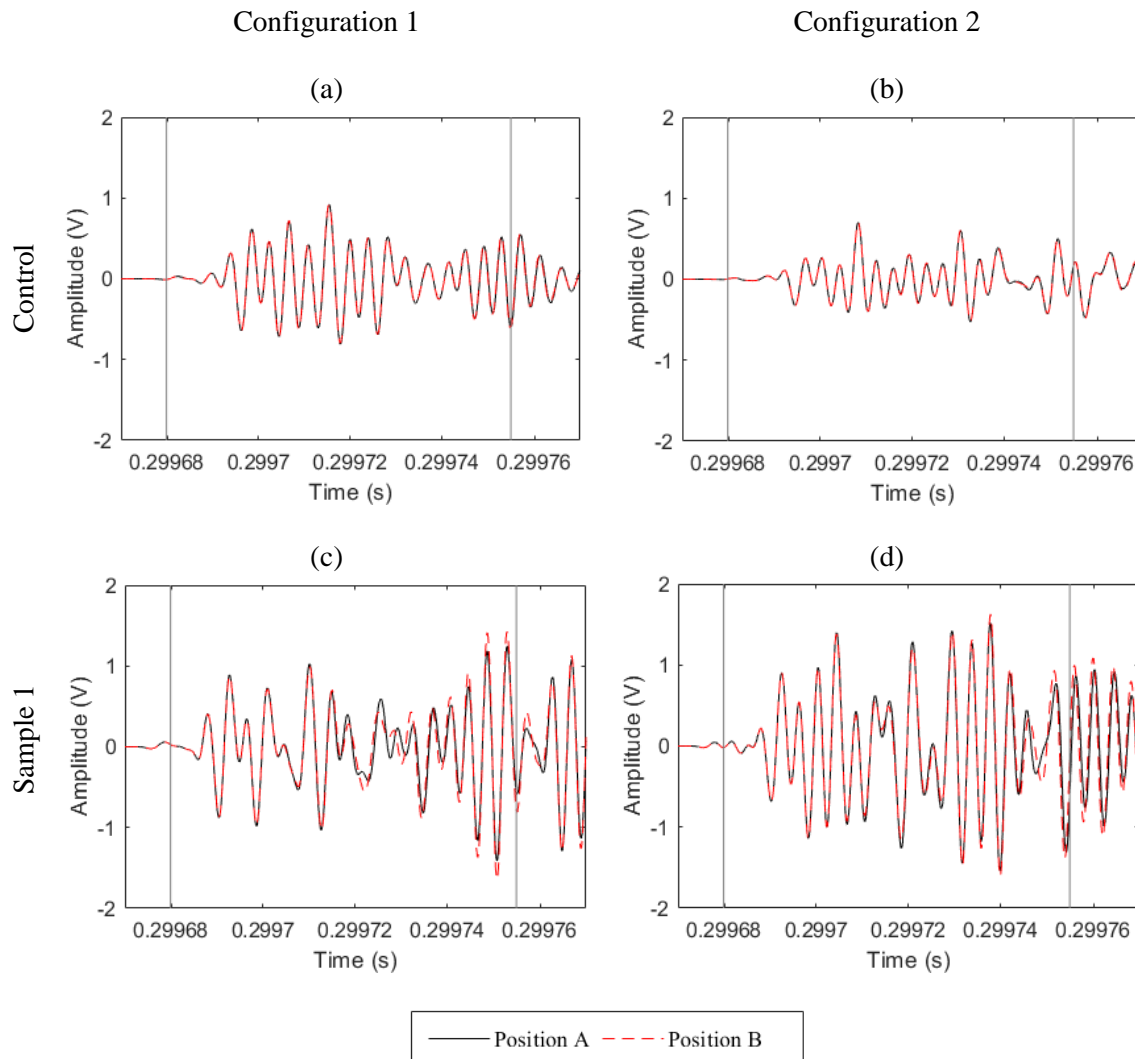
Figure 7 –. Superposition of reciprocal signals for the maximum amplitude (150V): the black solid line refers to the signal recorded in B when emitting from A, while the dashed red line refers to signals recorded in A when emitting from B. Plots in the first row (a and b) are signals detected in the Control sample (undamaged) and plots in the second row (c and d) are relative to the Sample 1 (damaged). The first column is the superposition of signals recorded in Configuration 1 (a and c) and the second column is the superposition of signals recorded in Configuration 2 (b and d). The vertical lines correspond to the windows applied for the signal analysis.

The data for the two configurations and all amplitudes can be analyzed to calculate the parameter D^i as defined in Eq. (3) and results are reported in Fig. 8. The vertical lines in Figure 7 correspond to the windows applied for the signal analysis of Figure 8, since this first part of the wave is not as much affected by the reflections and interactions with the material.

First, notice that the nonlinearity of the response is given by the break of the superposition principle, i.e., the higher the input amplitude is, the less reciprocal the signals are (larger differences in the signals).

The Control sample shows low values in all cases even for the higher excitation amplitudes, while damaged samples reveal higher D values. However, in both configurations, Sample 4 exhibited values very close to the Control sample and Sample 3 showed values under Samples 1 and 2, which were less damaged (see

Section 2.2.). This could have been because cracks were so wide that there was little non-linear interaction for the deformations that were being generated.

It is interesting for real in situ applications that the damaged samples with non-visible cracks give higher values and are able to discriminate the presence of damage.
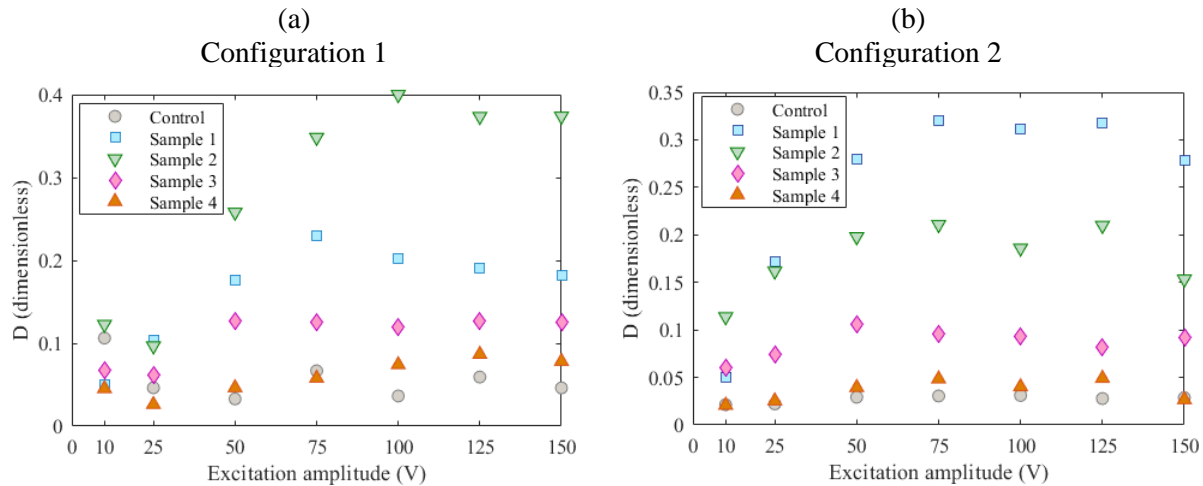
Figure 8 –. Reciprocity indicator, D, versus the input amplitude for all the samples: (a) Configuration 1 and (b) Configuration 2.

4   Conclusions

The results obtained in this study indicate that the ultrasonic waves traveling through the reinforced cement mortar specimens clearly increase their non-linear character in the course of accelerated steel corrosion tests. The evolution of values found in this work for the Intensity Modulation Ratio (R), seems to indicate that the nonlinear features may be appearing before the observation of a visible crack. The appearance of microcracks leads to an increase in non-linearity of the signal: intermodulation products and break of reciprocity principle. The parameter D seems to be useful to detect damage at early stages. As a result, it is possible to use non-linear ultrasonic techniques for the detection of cracks due to the corrosion of the embedded steel bar in reinforced concrete or mortar model specimens.

Acknowledgments

References

[1] P. Antonaci, C.L.E. Bruno, M. Scalerandi, F. Tondolo, Effects of corrosion on linear and nonlinear elastic properties of reinforced concrete, Cement and Concrete Research 51 (2013) 96-103.

[2] M. Korenska, M. Matysik, P. Vyroubal, K. Pospisil, Assessment of reinforcement corrosion using nonlinear ultrasonic spectroscopy, 5th NDT Progress–International Workshop of NTD Experts. Prague, 2009.

[3] D.M. Donskoy, K. Ferroni, A. Sutin, K. Sheppard, A nonlinear acoustic technique for crack and corrosion detection in reinforced concrete, Nondestructive Characterization of Materials Viii (1998) 555-560.

[4] M. Miró, J.N. Eiras, P. Poveda, M.-Á. Climent, J. Ramis, Detecting cracks due to steel corrosion in reinforced cement mortar using intermodulation generation of ultrasonic waves, Construction and Building Materials 286 (2021) 122915.

[5] C. Woodward, M.N. Amin, Evaluating rebar corrosion using nonlinear ultrasound, 34th Annual Review of Progress in Quantitative Nondestructive Evaluation, Amer Inst Physics, Golden, CO, 2007, pp. 1314-1319.

[6] M.A. Climent-Llorca, M. Miro-Oca, P. Poveda-Martinez, J. Ramis-Soriano, Use of Higher-Harmonic and Intermodulation Generation of Ultrasonic Waves to Detecting Cracks due to Steel Corrosion in Reinforced Cement Mortar, International Journal of Concrete Structures and Materials 14(1) (2020) 17.

[7] M.Á. Climent, M. Miro, J. Carbajo, P. Poveda, G. de Vera, J. Ramis, Use of Non-Linear Ultrasonic Techniques to Detect Cracks Due to Steel Corrosion in Reinforced Concrete Structures, Materials 12(5) (2019).

[8] K.E.A. Van den Abeele, P.A. Johnson, A. Sutin, Nonlinear elastic wave spectroscopy (NEWS) techniques to discern material damage, part I: Nonlinear wave modulation spectroscopy (NWMS), Research in Nondestructive Evaluation 12(1) (2000) 17-30.

[9] H.C. Wu, K. Warnemuende, How cracks modulate nonlinear acoustic signals C3 - 11th International Conference on Fracture 2005, ICF11, 2005, pp. 1560-1565.

[10] D. Donskoy, A. Sutin, A. Ekimov, Nonlinear acoustic interaction on contact interfaces and its use for nondestructive testing, Ndt & E International 34(4) (2001) 231-238.

[11] L. Pieczonka, A. Klepka, A. Martowicz, W.J. Staszewski, Nonlinear vibroacoustic wave modulations for structural damage detection: an overview, Optical Engineering 55(1) (2016).

[12] P. Antonaci, C.L.E. Bruno, A.S. Gliozzi, M. Scalerandi, Monitoring evolution of compressive damage in concrete with linear and nonlinear ultrasonic methods, Cement and Concrete Research 40(7) (2010) 1106-1113.

[13] B.A. Auld, Acoustic fields and waves in solids. Vol.1, Acoustic fields and waves in solids. Vol.1 (1973) v+423 pp-v+423 pp.

[14] J.D. Achenbach, Reciprocity in elastodynamics, Cambridge University Press2003.

[15] O.A. Godin, Reciprocity and energy conservation within the parabolic approximation, Wave motion 29(2) (1999) 175-194.

[16] J. Porto, R. Carminati, J.-J. Greffet, Theory of electromagnetic field imaging and spectroscopy in scanning near-field optical microscopy, Journal of Applied Physics 88(8) (2000) 4845-4850.

[17] P. Leung, R. Chang, Reciprocity in nonlocal nano-optics, Journal of Optics A: Pure and Applied Optics 10(7) (2008) 075201.

[18] M. Scalerandi, C.L.E. Bruno, A.S. Gliozzi, P.G. Bocca, Break of reciprocity principle due to localized nonlinearities in concrete, Ultrasonics 52(6) (2012) 712-719.

[19] C. Athanasiadis, I. Stratis, V. Sevroglou, N. Tsitsas, Point-source elastic scattering by a nested piecewise homogeneous obstacle in an elastic environment, Mathematics and mechanics of solids 15(4) (2010) 419-438.

[20] J.D. Tippmann, X. Zhu, F.L. di Scalea, Application of damage detection methods using passive reconstruction of impulse response functions, Philosophical Transactions of the Royal Society a-Mathematical Physical and Engineering Sciences 373(2035) (2015) 17.

[21] UNE-EN:197-1, Cemento. Parte 1: Composición, especificaciones y criterios de conformidad de los cementos comunes, AENOR, Spain, 2011.

[22] M.A. Climent, G. de Vera, E. Viqueira, M.M. Lopez-Atalaya, Generalization of the possibility of eliminating the filtration step in the determination of acid-soluble chloride content in cement and concrete by potentiometric titration, Cement and Concrete Research 34(12) (2004) 2291-2295.

[23] ASTM:G1-03, Standard practice for preparing, cleaning, and evaluating corrosion test specimens, ASTM, Philadelphia, Pennsylvania, 2004, p. 9 p.

[24] UNE-EN:196-1, Métodos de ensayo de cementos. Parte 1: Determinación de resistencias, AENOR, Spain, 2018.

[25] G. Nossoni, R. Harichandran, Current Efficiency in Accelerated Corrosion Testing of Concrete, Corrosion 68(9) (2012) 801-809.

[26] Dakel., IDK09. http://www.dakel.cz. (Last consulted: October 2020)).

[27] OLYMPUS, Model 5058PR High Voltage Pulser-Receiver. https://www.olympus-ims.com/en/downloads/detail/?0[downloads][id]=276824180. (Accessed August 2021).

[28] J. Chen, A.R. Jayapalan, J.-Y. Kim, K.E. Kurtis, L.J. Jacobs, Rapid evaluation of alkali-silica reactivity of aggregates using a nonlinear resonance spectroscopy technique, Cement and Concrete Research 40(6) (2010) 914-923.